ON THE CORONAL LINES IN THE CHROMOSPHERE AT THE 1970 ECLIPSE

M. KANNO
Hida Observatory, University of Kyoto, Kamitakara, Gifu-Ken, Japan
T. TSUBAKI
Institute of Earth Science and Astrophysics, University of Shiga, Ohtsu, Japan
and
H. KUROKAWA
Kwasan Observatory, University of Kyoto, Yamashina, Kyoto, Japan

(Received 21 June, 1971)

Abstract. Spectrographic observations of the flash spectrum were made by the Kwasan Observatory at the total solar eclipse on 7 March, 1970. The integrated intensities of Fe XIV λ5303, Fe X λ6374, and the continuum were measured on the spectrograms as a function of height above the Sun's limb. It was found that a large amount of emission in the coronal lines originates in the interspicular regions of the chromosphere. Analysis of the data yielded that the interspicular regions consist of coronal material of $T_e = 1.6 \times 10^6$–1.2×10^6 and $\log N_e = 8.5$–9.5, and that a decrease in T_e and an increase in N_e occur with decreasing height.

1. Introduction

It is well known that the spicules are the essential element of the upper chromosphere higher than 1000 km or so, where chromospheric emissions such as H, He, He^+, and Ca^+ are confined to the spicules. However, there is little knowledge on the physical conditions in the interspicular regions. Athay and Roberts (1955) measured the intensities of coronal lines and continuum as a function of height on the slitless spectrograms at the 1952 eclipse. Although the data were not accurate enough to give the detailed shapes of the eclipse curves, they concluded that the maximum surface brightness in Fe XI λ7892 occurs below 10 000 km and that the coronal line emission begins to be important near the top of the chromosphere, perhaps even in the regions between the spicules. At the 1966 eclipse Weart (1968) made the photoelectric observations of the coronal lines Fe XIV λ5303 and Fe X λ6374 in heights below 10 000 km. He found that the surface brightness of the coronal lines is, so far as the photon shot noise allows us to tell, constant throughout the region studied, and concluded that coronal activity and its associated emission extend far below the top of the spicules. These eclipse results imply the fact that coronal material extends down into the chromospheric heights (the interspicular regions), which is in accordance with indirect indications from visible, radio, and EUV spectra (e.g. Moriyama, 1961; Suemoto and Moriyama, 1963, 1964; Athay, 1963; Zirin and Dietz, 1963).

In order to infer the physical conditions in the interspicular regions below 10 000 km, we made spectrographic observations of the flash spectrum involving the green and red coronal lines at the total solar eclipse of 7 March, 1970 at Puerto Escondido,

Solar Physics **21** (1971) 314–324.

Mexico. We measured the integrated intensities of $\lambda 5303$, $\lambda 6374$, and the continuum as a function of height above the Sun's limb, which were analyzed to determine electron temperature and electron density in the interspicular regions.

2. The Observations

Observations were made with a slot spectrograph having an image-forming system. A coelostat and an objective lens with a 30-cm effective aperture and 459-cm focal length produced a Sun's image of 43.1-mm diameter on the entering focal plane where a wide slot was located to cut off the light from the opposite limb of each contact point. The light through a collimating lens of 14-cm diameter and 70-cm focal length fell on a grating of 600 grooves/mm, which produced a spectrum with an average plate dispersion of 19 Å/mm. For the spectrum from 4650 to 6800 Å, an aerial camera was placed behind an imaging lens of 14-cm diameter and 70-cm focal length. Eastman Kodak Tri-X Aerecon film was used in this spectral range. The spectral images were minified by about one third in the direction of dispersion to reduce photometric errors in measuring broad coronal lines.

Several exposures for the partial Sun were made from 70 s to 60 s before second contact, which were used for the calibration of absolute intensities by fitting to the limb darkening observations taken so far. Then the camera ran from 20 s before, till 40 s after second contact. The exposures for third contact were made in a reverse program to that of second contact. The exposure times of the flash spectra ranged 0.25 to 2.3 s and the interval for advance of film was less than 0.6 s. Then the height resolution of the spectra at contact point was about 220 km in heights below 2000 km, and about 760 km in greater heights. The standardization of the film for characteristic curves was made by step-attenuated spectrograms of the Sun taken after the eclipse. The zero point for the height scale was chosen in the usual way to be the point of inflection in the plot of specific intensity against height for the continuum at 6375 Å.

A more detailed description of our eclipse observations and the photometric procedures will be published elsewhere in the future.

3. Results of the Measurements

We chose two regions near the Sun's equator for measuring the integrated intensities of $\lambda 5303$, $\lambda 6374$, and the continuum. The regions are located on the west limb at the heliocentric position angle 236° (Point A) and 249° (Point E) which are indicated on the spectrogram in Figure 1. The direct photographs of white light corona taken by us during the mid-totality showed a moderately intense helmet above these regions. But the regions of the Sun's limb showed no sign of chromospheric activity on the eclipse day. (See the solar map of the Fraunhofer Institute.) Coronagraphic observations (Fisher *et al.*, 1970) showed that there was no noticeable activity in H_α and $\lambda 5303$ on the west limb during our eclipse observations. Thus the regions may be regarded as representative of the average chromosphere.

The continuum intensities, E_c (erg $s^{-1}cm^{-1}sterad^{-1}$ $Å^{-1}$), were measured at the

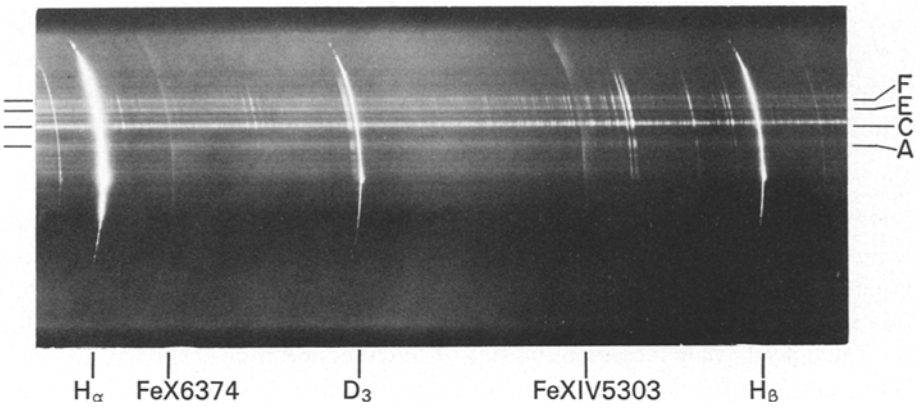

Fig. 1. A west-limb spectrogram, showing the points traced for the measurements of Fe XIV λ5303, Fe X λ6374, and the continuum.

wavelength near each coronal line. The values of log E_c at Point A are plotted against height in Figure 2, together with those of λ4700 at the 1952 eclipse by Athay *et al.* (1955), and of λ5278 at the 1966 eclipse by Weart (1968). There are no differences greater than 0.1 between the values of log E_c at Point A and those at Point E. It is seen from Figure 2 that although these eclipse data show a very similar shape in log E_c-versus-height curves, our absolute intensity is about 1.5 times lower than the

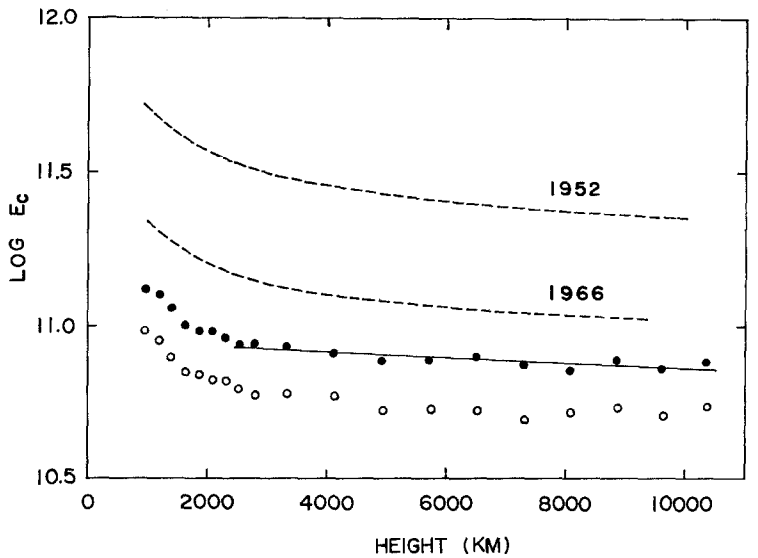

Fig. 2. The continuum intensities at λ5303 (solid circles) and at λ6374 (open circles) in Point A, which are compared with the 1952 data at λ4700 (upper dashed line) of Athay *et al.* (1955) and the 1966 data at λ5278 (lower dashed line) of Weart (1968). The solid line represents the empirical expression of Equation (1).

others (when the 1952 data are reduced by a factor of 2). This may be partly attributed to real variations of the continuum intensities in time as well as in position on the solar limb.

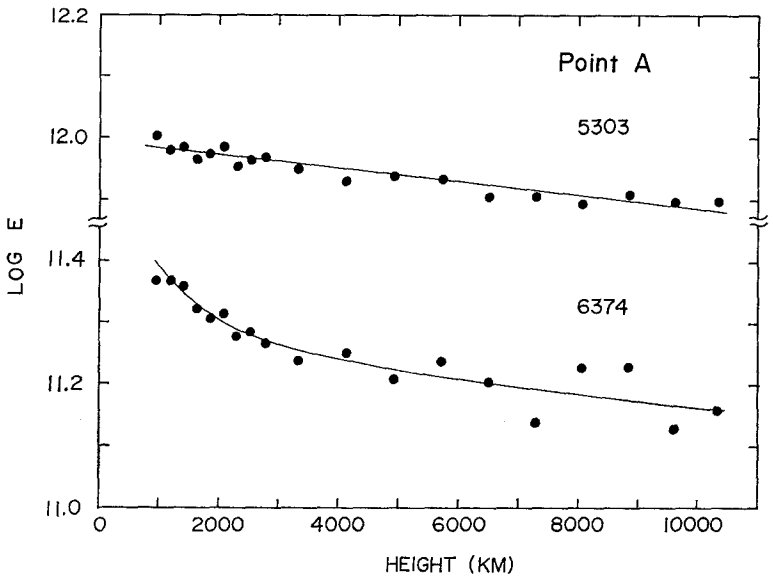

Fig. 3. The integrated intensities of Fexiv λ5303 and Fex λ6374 at Point A. The solid lines represent the empirical expressions of Equations (5) and (6).

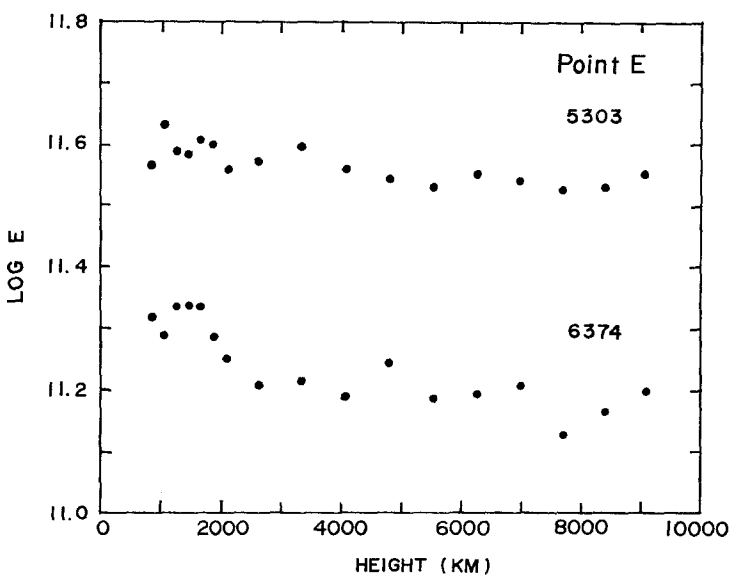

Fig. 4. The integrated intensities of Fexiv λ5303 and Fex λ6374 at Point E.

The microdensitometer tracings for the lines λ5303 and λ6374 were made on all the spectrograms of third contact. The line profiles of the coronal lines on the tracings present broad features even in the minified spectral images, and extend over the wavelength range of ≈30 Å in λ5303 and ≈19 Å in λ6374. These correspond to the height range of ≈130 000 km and ≈80 000 km above the Moon's limb, respectively. In order to reduce random errors arising from uncertainty of the profiles at the far wings, we adopted an average value of all spectrograms for the values of integration over the wing portion above the chromospheric height of 50 000 km for λ5303 and 40 000 km for λ6374.

The integrated intensities of the coronal lines, E (erg $s^{-1}cm^{-1}sterad^{-1}$), are shown as a function of height in Figures 3 (Point A) and 4 (Point E). No measurements were made for the heights below 800 km, because the coronal lines show effects of blending with chromospheric lines. It is found from Figures 3 and 4 that the intensities

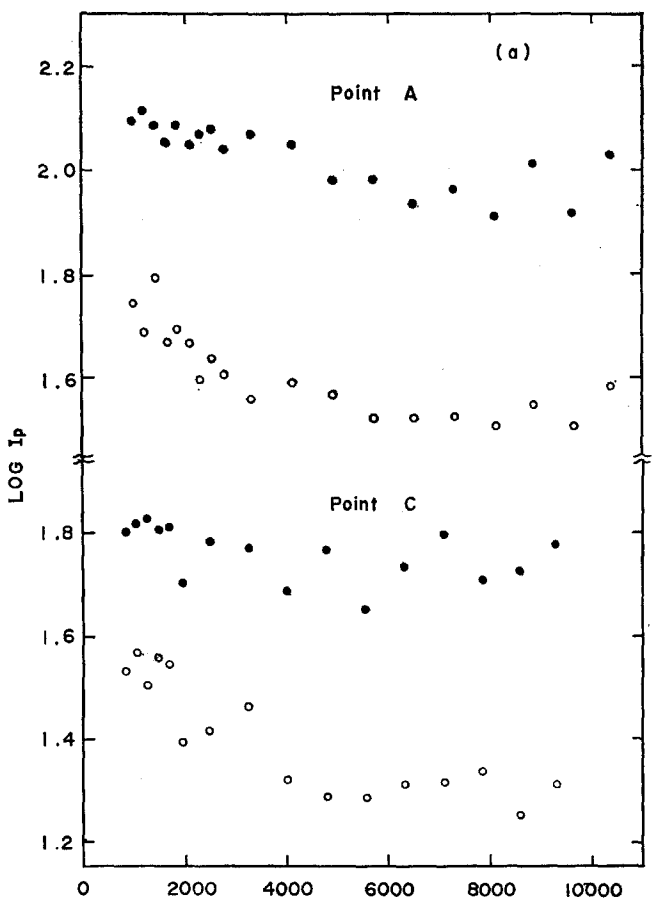

Figs. 5a–b. The peak intensities of Fe XIV λ5303 (solid circles) and Fe X λ6374 (open circles) in an arbitrary unit at Points A, C, E, and F, which may be considered to be a good measure of the integrated intensities.

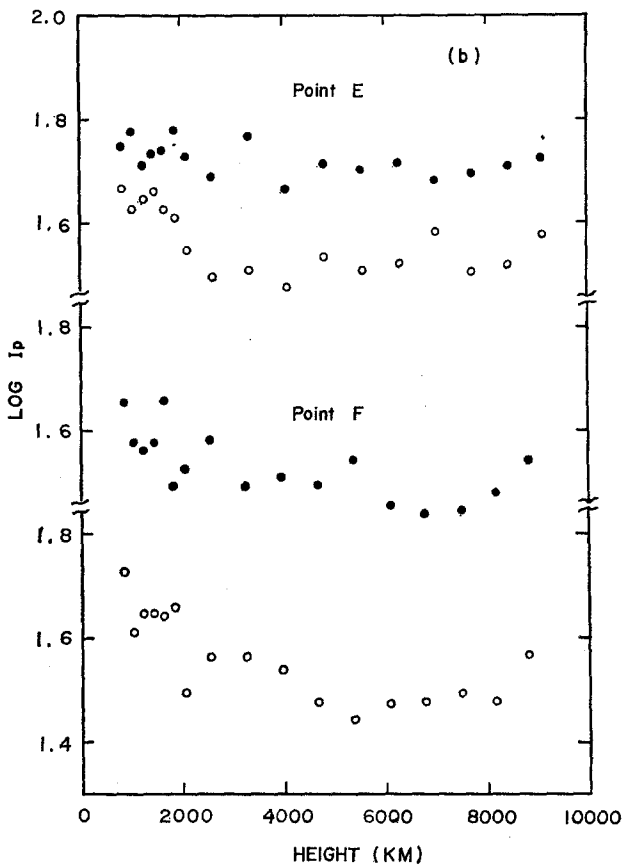

Fig. 5b.

of $\lambda 5303$ and $\lambda 6374$ are increasing to the heights as low as 1000 km, and especially the line $\lambda 6374$ shows a marked intensification below 3000 km. In order to obtain further evidences for these results, we measured the intensities at the peak of the line profiles, I_p, at other two regions on the west limb; Point C (P.A. $=243°$) and Point F (P.A. $=253°$), which are shown in Figure 1. Since the line widths of the coronal lines at each point show no appreciable variations with height, I_p can be regarded as a good measure of the integrated intensities of the coronal lines. Values of $\log I_p$ at Points A, C, E, and F are shown in an arbitrary unit against height in Figures 5(a) and (b). It is seen from these figures that at all points measured, the peak intensities of $\lambda 5303$ and $\lambda 6374$ are increasing with decreasing height and those of $\lambda 6374$ show a marked increase in low heights as well as the integrated intensities at Points A and E, though the absolute values of I_p considerably vary with the position on the Sun's limb. Since this behavior of $\lambda 5303$ and $\lambda 6374$ may be considered to be independent of the position angle, we can safely ignore the possibility of any localized emission centers in the corona lying in the line of sight.

Thus we conclude that coronal emission actually arises from the interspicular

regions of the chromosphere and that the maximum surface brightness in the coronal lines occurs near the base of the interspicular regions. Our results are in accordance with the previous eclipse observations by Athay and Roberts (1955) and by Weart (1968), except that the values of $\log E_{6374}$ significantly increase in low heights. We believe that this increase in $\log E_{6374}$, being beyond the limit of observational errors, reflects real effects in the interspicular regions.

4. Analysis of the Data

We will use the data in the preceding section to estimate electron density, N_e, and electron temperature, T_e, in the interspicular regions of the chromosphere. Since effects of self-absorption are unimportant for the coronal lines and the continuum, we can directly find volume emissivities from the $\log E$-versus-height curves, which yield values of N_e and T_e as a function of height. The data of Points A and E exhibit a similar variation with height, so that we will analyze the data of Point A as a typical region.

Since electron scattering of photospheric radiation becomes important above 1000 km, an analysis of the continuum data will give the density structure in large heights. The height gradient of the continuum intensities is very small in heights $h > 2500$ km as seen in Figure 2, so that we assume that most of emission in the continuum comes from the interspicular regions in these heights. The continuum data at $\lambda 5303$ of Point A above 2500 km were fitted with a single exponential term by a least-squares method:

$$E_c = 8.98 \times 10^{10} \exp(-2.04 \times 10^{-10} h), \tag{1}$$

which is shown by the solid line in Figure 2. Assuming a spherically symmetric atmosphere, we have the volume emissivity of the continuum, ε_c (erg s^{-1} cm^{-3} sterad^{-1} Å^{-1}):

$$\varepsilon_c = 3.95 \times 10^{-10} \exp(-2.04 \times 10^{-10} h). \tag{2}$$

If we assume that the continuum arises from electron scattering, we have

$$\varepsilon_c = \tfrac{1}{2} J_\lambda N_e \sigma_e, \tag{3}$$

where J_λ is the mean monochromatic intensity at the solar surface and σ_e is the coefficient of electron scattering. Adopting the values of $J_{5303} = 2.94 \times 10^6$ and $\sigma_e = 0.665 \times 10^{-24}$ (Allen, 1963), we obtain from Equations (2) and (3)

$$\log N_e = 8.61 - 0.885 \times 10^{-10} h. \tag{4}$$

Since we have not taken into account the continuum data in low heights, this equation should be applicable only to higher levels of the interspicular regions. Equation (4) gives values of N_e nearly constant throughout the observed heights below 10 000 km.

In the height range of the observations the data of the line $\lambda 5303$ at Point A can be represented, to within the allowed accuracy, by a single exponential term fitted by least squares:

$$E_{5303} = 9.78 \times 10^{11} \exp(-2.44 \times 10^{-10} h). \tag{5}$$

For the data of the line $\lambda 6374$ we adopted a representation in terms of a sum of two exponential terms. A least-squares fit to the data at Point A gives the equation:

$$E_{6374} = 1.95 \times 10^{11} \exp(-2.96 \times 10^{-10} h) + \\ + 1.88 \times 10^{11} \exp(-1.26 \times 10^{-8} h), \tag{6}$$

where the first term represents the straight-line portion of the $\log E_{6374}$-curve above 4000 km and the second term corresponds to the increase of the intensity at low heights. The empirical curves of Equations (5) and (6) are shown by the solid lines in Figure 3.

On the assumption of a spherically symmetric atmosphere, Equations (5) and (6) give the volume emissivities ε (erg s^{-1} cm^{-3} $sterad^{-1}$) of $\lambda 5303$ and $\lambda 6374$:

$$\varepsilon_{5303} = 5.66 \times 10^{-9} \exp(-2.44 \times 10^{-10} h), \tag{7}$$

and

$$\varepsilon_{6374} = 1.50 \times 10^{-9} \exp(-2.29 \times 10^{-10} h) + \\ + 4.00 \times 10^{-7} \exp(-1.26 \times 10^{-8} h). \tag{8}$$

For the forbidden coronal lines $\lambda 5303$ and $\lambda 6374$, the volume emissivity may be represented in the form

$$\varepsilon = \frac{h\nu}{4\pi} 0.8 N_e (A_{lu} + C_{lu} + \sum C_{lk} P_{ku}) \frac{N(\mathrm{Fe})}{N(\mathrm{H})} \frac{N(\mathrm{ion})}{N(\mathrm{Fe})}, \tag{9}$$

where A_{lu} is the rate of radiative excitation, C_{lu} is the rate of direct collisional excitation, $\sum C_{lk} P_{ku}$ is the rate of transitions involving the collisions to higher levels which are followed by cascade to the upper level of the forbidden line, and $N(\mathrm{H})$, $N(\mathrm{Fe})$, and $N(\mathrm{ion})$ are the number densities of hydrogen, iron, and the iron ion in question, respectively. In Equation (9) we have assumed $N(\mathrm{H})/N_e = 0.8$, and taken into account the three mechanisms which lead to excitation of ions populating the upper level of the coronal line. We computed the numerical values of A_{lu}, C_{lu}, and $\sum C_{lk} P_{ku}$ for various combinations of N_e and T_e according to Pottasch (1964a). Although the quantity $R = A_{lu} + C_{lu} + \sum C_{lk} P_{ku}$ is a function of N_e and T_e, the ratio R_{5303}/R_{6374} is rather insensitive to N_e and T_e. Thus we can find values of T_e from the ratio $\varepsilon_{5303}/\varepsilon_{6374}$, if the relative population of ions are known as a function of T_e. For the values of $N(\mathrm{ion})/N(\mathrm{Fe})$, we adopted the results of ionization equilibrium calculations by Jordan (1969) which include the processes of dielectronic recombination and collisional excitations followed by autoionization. Using the values of T_e determined above, we can obtain values of N_e from Equations (7) or (8), and (9). As to the relative abundance

of iron, we adopted the value of $N(\mathrm{Fe})/N(\mathrm{H}) = 4 \times 10^{-5}$ obtained from the EUV line analysis by Pottasch (1964b). Figure 6 exhibits the final results of T_e and N_e distributions with height yielded from the coronal line data at Point A.

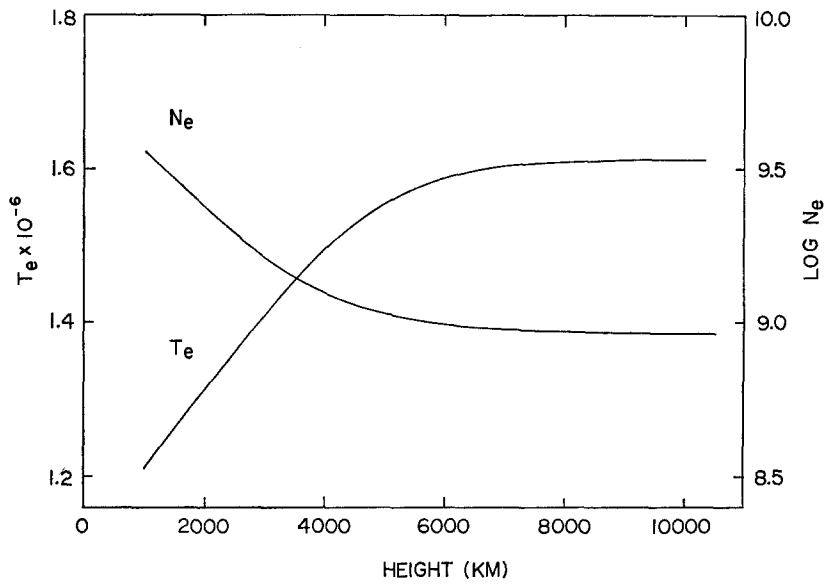

Fig. 6. The height distributions of T_e and N_e deduced from the data of the coronal lines at Point A. (Note that the continuum data give lower values of N_e, cf. Equation (4).)

It is seen from Figure 6 that the interspicular regions below 10 000 km consist of coronal material with $T_e = 1.6 \times 10^6$–1.2×10^6, and that there occur a decrease in T_e and an increase in N_e with decreasing height. We may now understand why a marked increase of log E_{6374} appears at lower heights. The higher levels of the interspicular regions have temperatures at which Fe XIII and Fe XIV are the most abundant ions of iron. The decrease in T_e at low heights produces such a change in the relative abundance of iron ions that Fe X becomes much more abundant than Fe XIV. The increase of N_e brings about a further increase in the volume emissivity of Fe X λ6374. Meanwhile, the volume emissivity of Fe XIV λ5303 is kept nearly constant with height, owing to inverse nature of both effects. The T_e-versus-height curve in Figure 6 shows that the temperature gradient around $T_e = 1.4 \times 10^6$ is about 1×10^{-3} deg cm^{-1}. This is of the same order of magnitude as those deduced from the EUV line analyses by Athay (1966) and by Dupree and Goldberg (1967), when we assume $N(\mathrm{Si})/N(\mathrm{H}) = 1 \times 10^{-4}$ and correct the Athay's results for the effects of dielectronic recombination.

Values of N_e at higher levels obtained from the coronal line data are greater than those from the continuum data (Equation (4)) by about 0.4 in the logarithm. This difference may be partly attributed to uncertainties of the rate coefficients of excitation and of the relative abundance of iron, appearing in Equation (9). But we must be cautious about the fact that our analysis relies on a double differentiation of the data,

and we should not give much weight to this difference. Then we conclude that $\log N_e = 8.5$–9.5 in the interspicular regions. If we assume the iron abundance of Goldberg *et al.* (1960), the coronal line data will give an order of magnitude greater values of N_e than those from the continuum data, so that our data are consistent with the coronal abundance of iron obtained by Pottasch (1964b).

In the above analysis we have ignored any effects of the spicules. If the fractional volumes occupied by spicules reach an appreciable amount in the low levels of the interspicular regions, it should be necessary to make some corrections to the volume emissivities obtained above. Furthermore it should be noticed that any fine details in the height distributions of T_e and N_e, particularly in greater heights, strongly depend on accuracy of the observed data. However, the overall nature of the present results is consistent with the prevailing picture that above a height of 1000 km or so, the chromosphere consists exclusively of spicules embedded in coronal material.

Finally, we discuss the data at Point E. Although Point E gives nearly same values of $\log E_{6374}$ as those at Point A, the differences in $\log E_{5303}$ amount to about 0.4. If we decrease the values of $\log \varepsilon_{5303}/\varepsilon_{6374}$ at Point A by 0.4, we will obtain a decrease in T_e of only 1×10^5 in all heights. As the volume emissivities of the coronal lines are nearly proportional to N_e^2, the differences in $\log N_e$ between Point A and Point E may be smaller than 0.2. Therefore we expect that the values of T_e and N_e at Point E are of the same order of magnitude as those at Point A. Thus the results of Point A may be regarded as typical ones of the interspicular regions of the chromosphere.

5. Conclusions

The 1970 eclipse observations indicated that the integrated intensities of Fe XIV λ5303 and Fe X λ6374 are increasing down to the height of about 1000 km above the Sun's limb, with a marked intensification in λ6374 below 3000 km. It is concluded that the interspicular regions in chromospheric heights below 10 000 km actually emit the coronal lines with relatively strong intensities per unit volume.

The analysis of the data at Point A yielded that the interspicular regions below 10 000 km are occupied by coronal material of $T_e = 1.6 \times 10^6$–1.2×10^6 and $\log N_e = 8.5$–9.5, and that there occur a decrease in T_e and an increase in N_e with decreasing height. These results may represent general features of the interspicular regions below 10 000 km, though there might be a little variety in the values of T_e and N_e with the position on the solar surface.

Acknowledgements

The authors wish to express their gratitude to the Ministry of Education which allowed the grants for the eclipse expedition to Mexico. They also wish to express their thanks to the Eclipse Committee of Japan (the Science Council of Japan) which gave cordial support to the eclipse expedition.

References

Allen, C. W.: 1963, *Astrophysical Quantities*, 2nd Ed., Athlone Press, London.
Athay, R. G.: 1963, *Astrophys. J.* **137**, 931.
Athay, R. G.: 1966, *Astrophys. J.* **145**, 784.
Athay, R. G., Menzel D. H., Pecker, J.-C., and Thomas, R. N.: 1955, *Astrophys. J. Suppl.* **1**, 505.
Athay, R. G. and Roberts, W. O.: 1955, *Astrophys. J.* **121**, 231.
Dupree, A. K. and Goldberg, L.: 1967, *Solar Phys.* **1**, 229.
Fisher, R. R., Pope, T., and Cain, S. D.: 1970, *Astrophys. Letters* **6**, 109.
Goldberg, L., Müller, E. A., and Aller, L. H.: 1960, *Astrophys. J. Suppl.* **45**, 1.
Jordan, C.: 1969, *Monthly Notices Roy. Astron. Soc.* **142**, 501.
Moriyama, F.: 1961, *Ann. Tokyo Astron. Obs., 2nd Ser.* **7**, 132.
Pottasch, S. R.: 1964a, *Monthly Notices Roy. Astron. Soc.* **128**, 173.
Pottasch, S. R.: 1964b, *Space Sci. Rev.* **3**, 816.
Suemoto, Z. and Moriyama, F.: 1963, *Space Research* **III** (ed. W. Priester), North-Holland Publishing Co., Amsterdam, p. 800.
Suemoto, Z. and Moriyama, F.: 1964, *Ann. Astrophys.* **27**, 775.
Weart, S. R.: 1968, Thesis, University of Colorado (JILA Report No. 96).
Zirin, H. and Dietz, R. D.: 1963, *Astrophys. J.* **138**, 664.